Electronic Supplementary Material (ESI) for New Journal of Chemistry.

Supporting Information

Functional Polyurethane-Urea Coatings from Sulfur Rich Hyperbranched Polymers and Evaluating Their Anticorrosion and Optical Properties

Nagaraj Goud Ireni,[1,3] Ramanuj Narayan,[1,3] Pratyay Basak,[,2,3] Kothapalli Venkata Suryanarayana Raju*[1,3]*

[1]Polymers and Functional Materials Division;

[2]Nanomaterials Laboratory, Inorganic & Physical Chemistry Division;

[3]Academy of Scientific & Innovative Research (AcSIR)

CSIR-Indian Institute of Chemical Technology (CSIR-IICT)

Hyderabad - 500 007, Telangana State, INDIA

Email: pratyay@iict.res.in; kvsnraju@iict.res.in

Tel(O): +91-40-27193225; Fax: +9140-27193991

*To whom all correspondences should be addressed

Characterisation of SHBPs

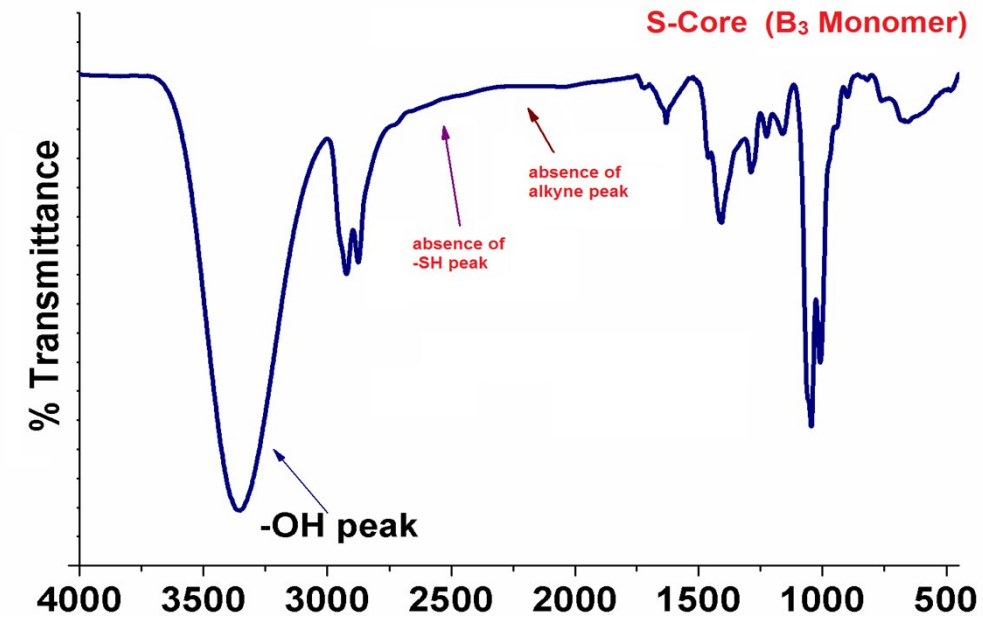

Figure SI-1(a). FTIR-spectra of S-Core (B_3 Monomer)

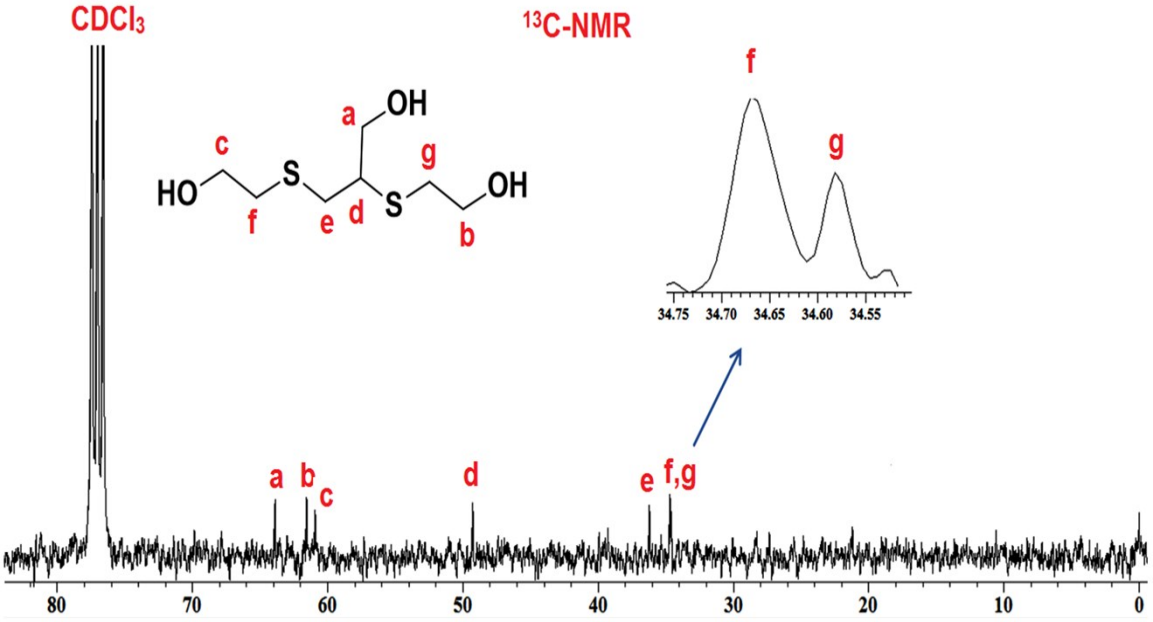

Figure SI-1(b). ^{13}C-NMR spectra of S-Core (B_3 Monomer)

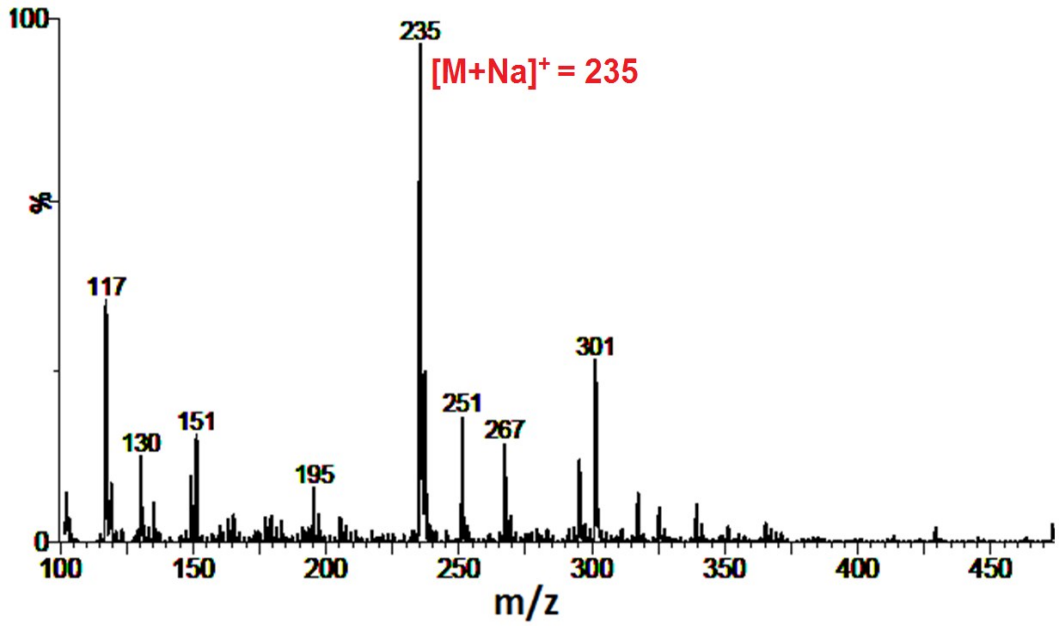

Figure SI-1(c). ESI-MS of S-Core (B_3 Monomer)

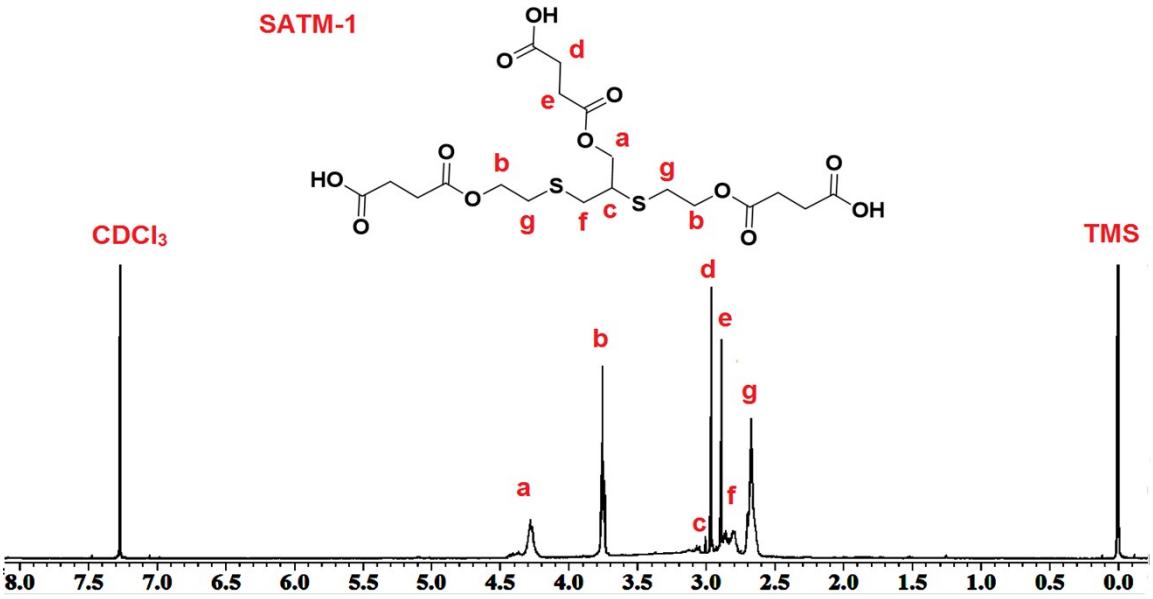

Figure SI-2(a). ^{1}H-NMR spectra of SATM-1

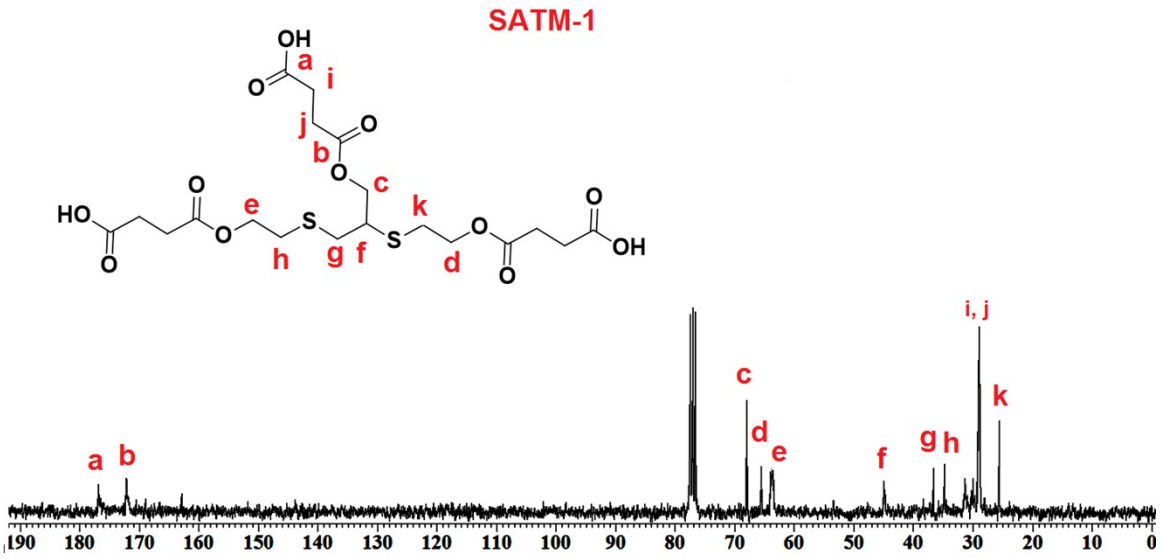

Figure SI-2(b). ^{13}C-NMR of SATM-1

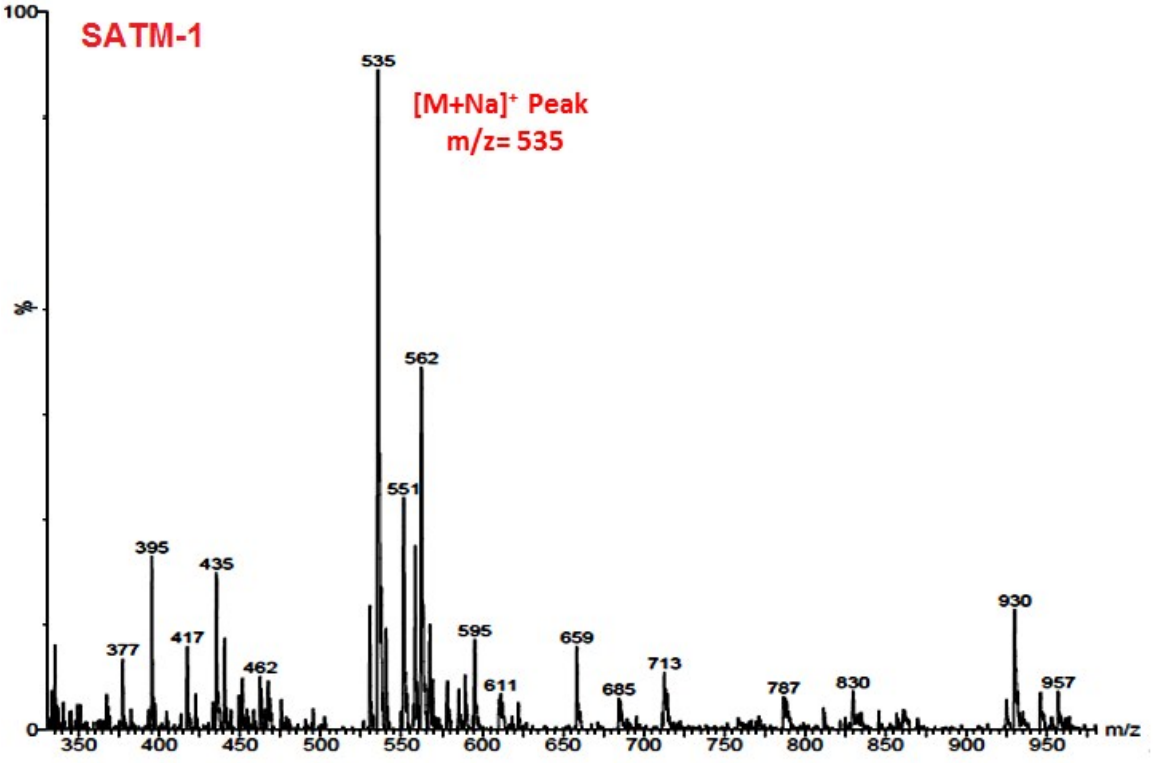

Figure SI-2(c). ESI-MS of SATM-1

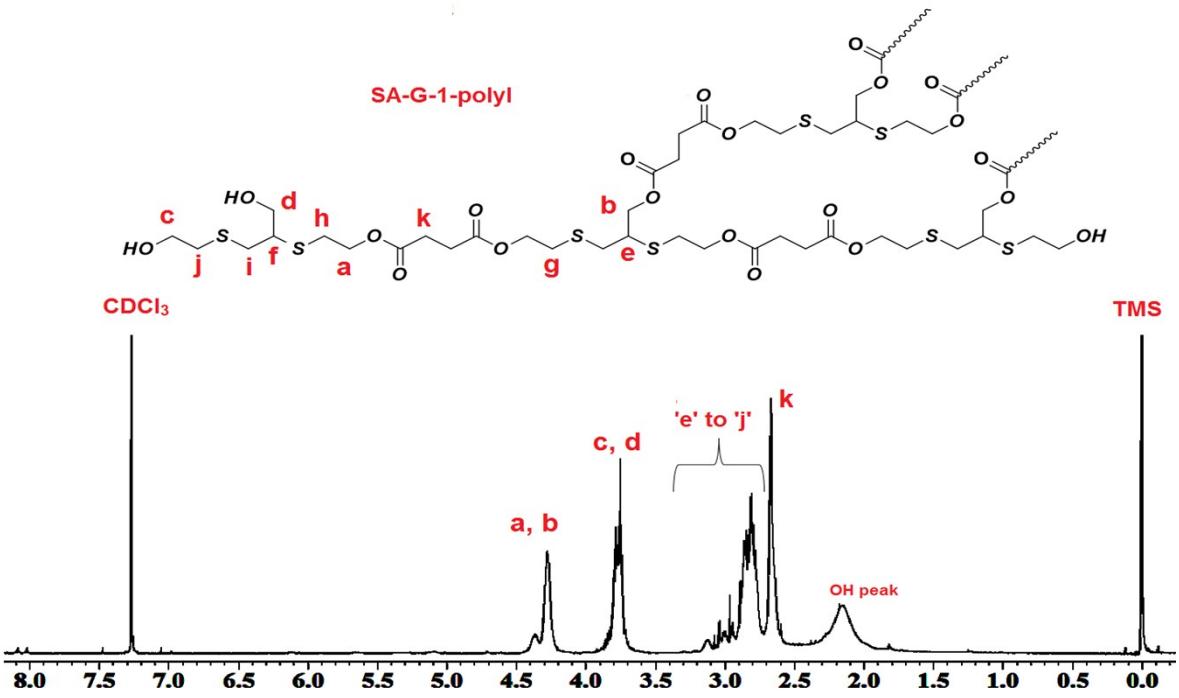

Figure SI-3(a). ^{1}H-NMR of SA-G-1-polyol

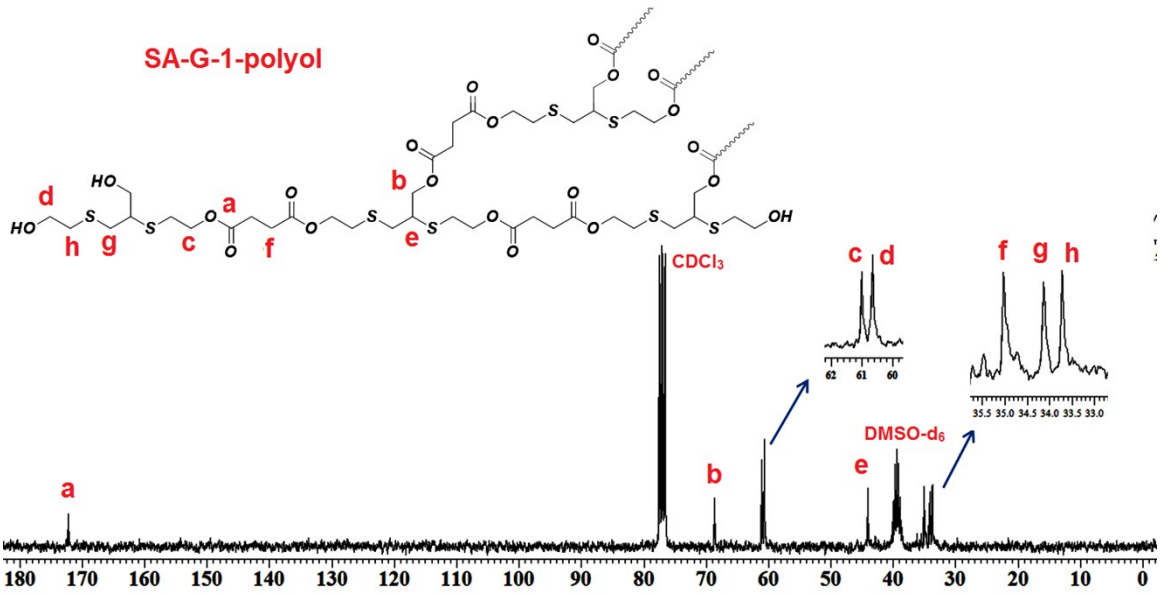

Figure SI-3(b). ^{13}C-NMR of SA-G-1-polyol

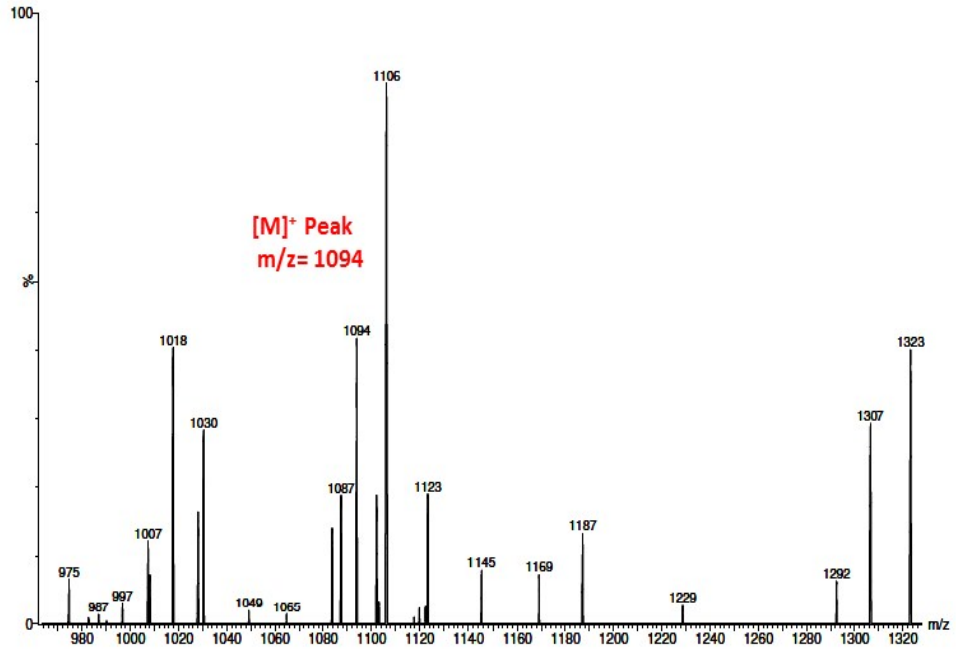

Figure SI- 3(c). ESI-MS of SA-G-1-polyol

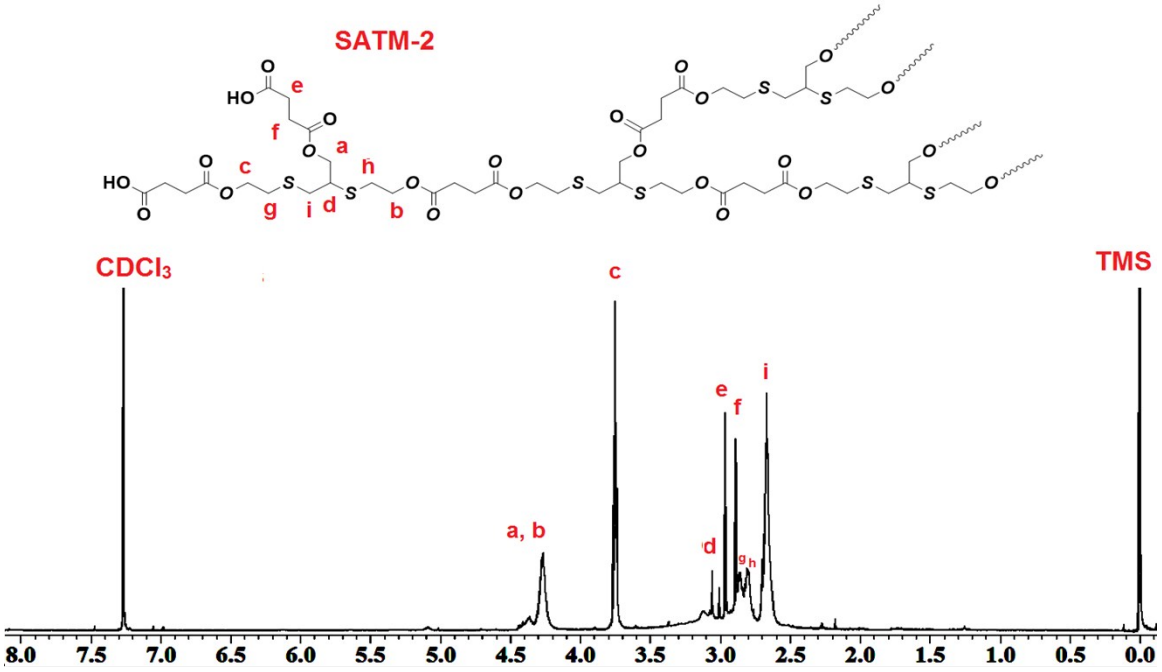

Figure SI-4 (a). ^{1}H-NMR of SATM-2

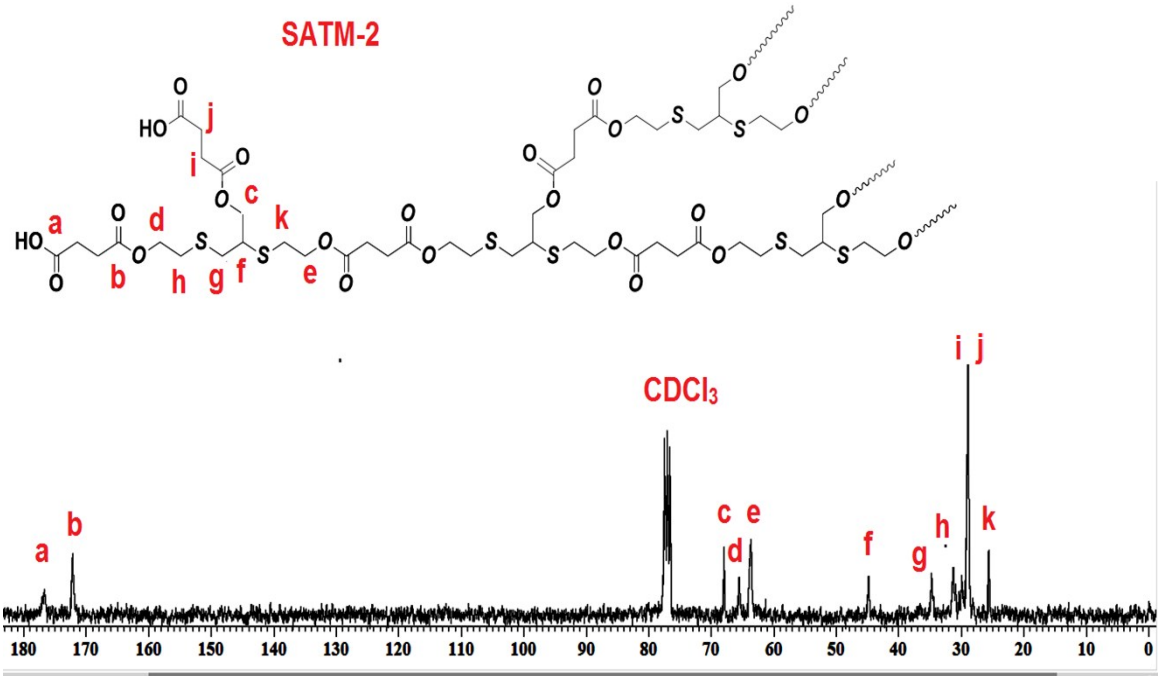

Figure SI-4 (b). ^{13}C-NMR of SATM-2

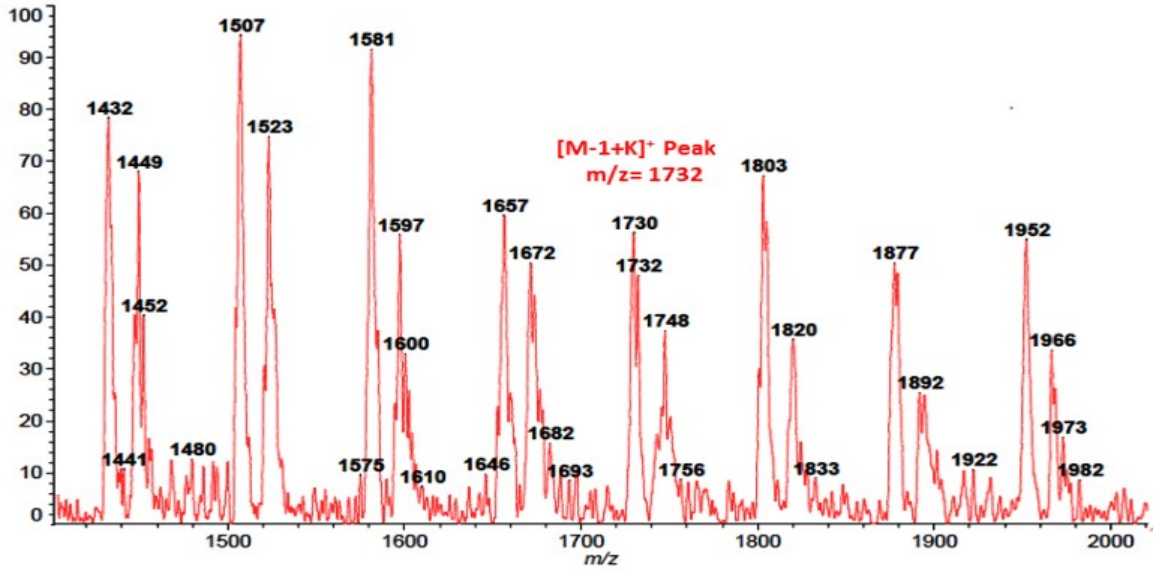

Figure SI-4(c). MALDI-TOF spectrum of SATM-2

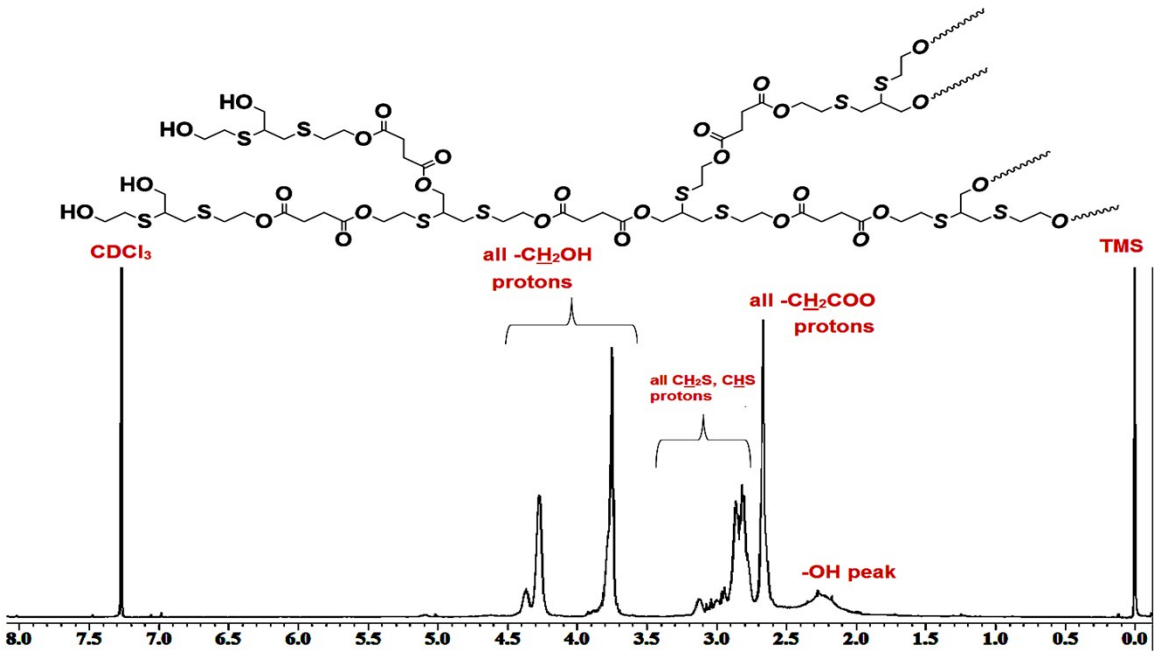

Figure SI-5 (a). ^{1}H- NMR of SA-G-2-polyol

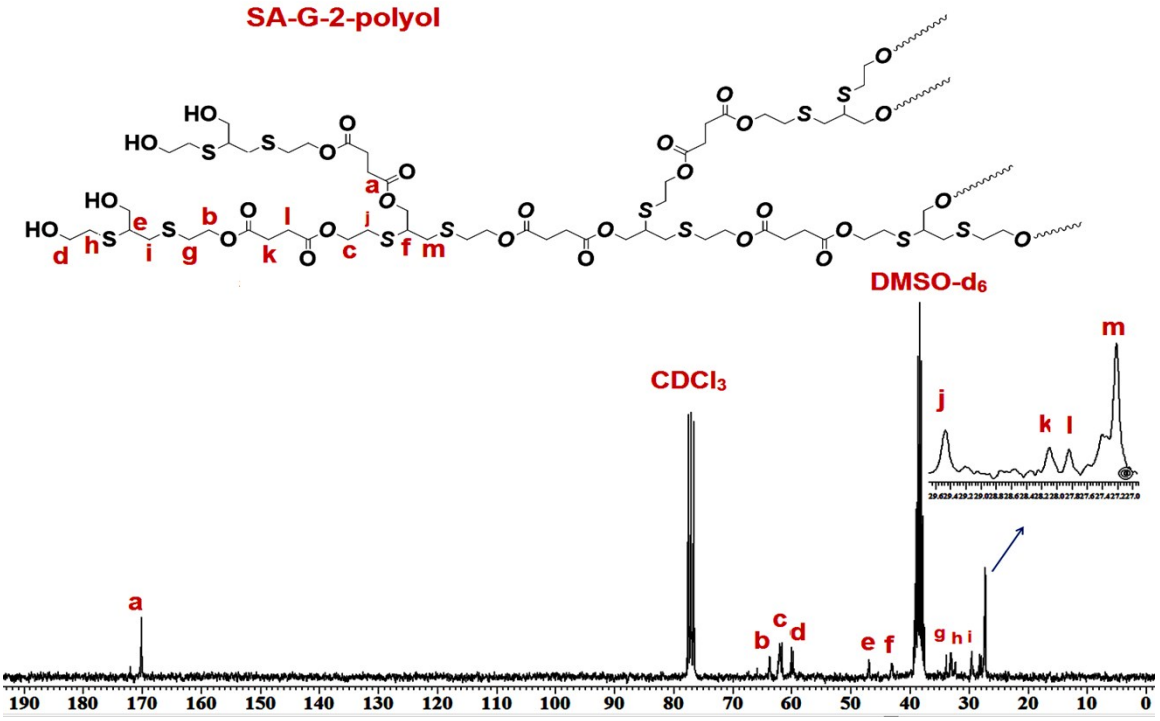

Figure SI-5(b). ^{13}C- NMR of SA-G-2-polyol

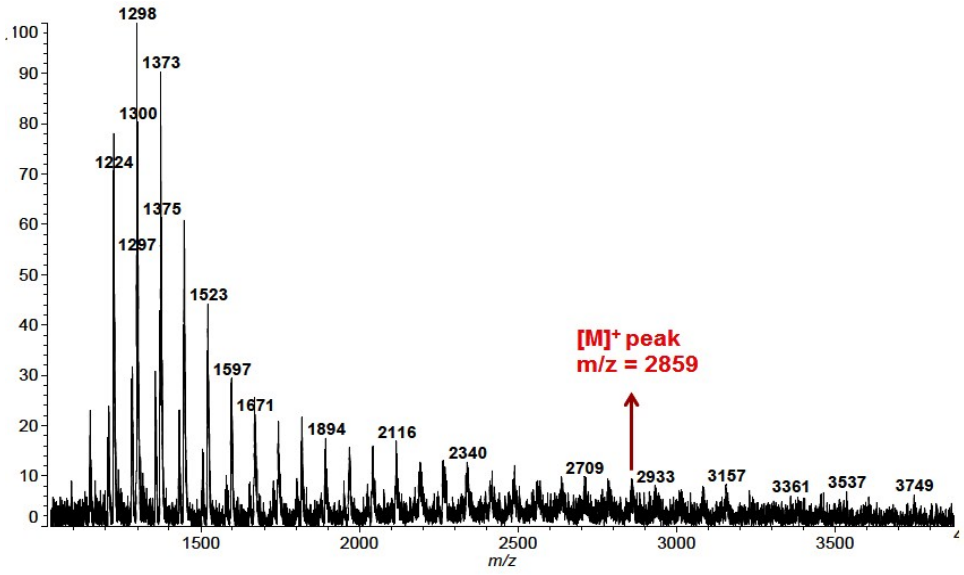

Figure SI 5(c). MALDI-TOF spectrum of SA-G-2-polyol

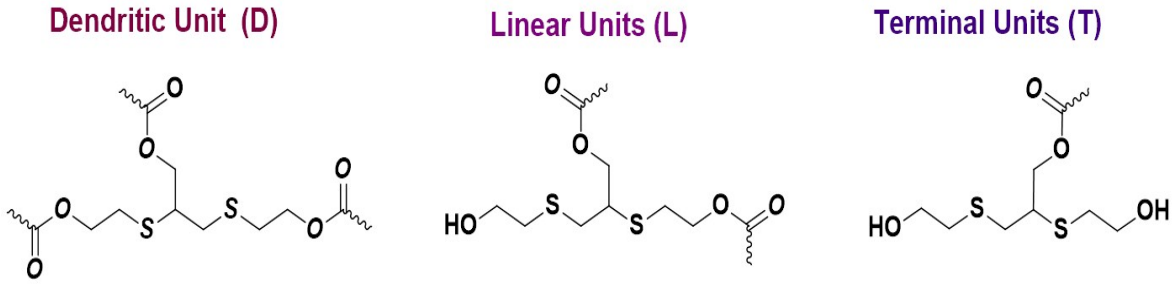

Figure SI-6. Schematic representation of possible dendritic (D), linear(L) and terminal (T) units of sulfur -rich HBPs for calculating the degree of branching (DOB).

Degree of branching (DB) **calculation.**

Typically, in HBPs, a combination of linear unreacted side-chains (L) coexists with dendritic segments (D) and terminal subunits (T). Identifying the fractional contribution of these dendritic, terminal and linear units provides a reasonable approximation on degree of branching (DB) expressed by the Frechet Equation: [1, 2]

$$DB = \frac{D + T}{D + L + T} \qquad (1)$$

Detailed analysis of ^{13}C-NMR was performed to assess the contributions of various subunits present in these sulfur-rich HBPs and estimate the degree of branching. According to the structural confirmations achieved, the tri-substituted S-Core monomer can be considered as dendritic units (D), while for di-esterified S-Core monomer as linear units, (L)and mono esterified units as terminal units (T).[3-6] The various possibilities of D, L and T units are provided in the **Figure SI-7.** For calculating DOB of these SHBPs we have utilized the C^{13}-NMR spectra of these polymers (see **SI-3(b)** and **SI-5(b)**) by concerning the ester carbonyl carbon.

All the subunits could be identified and assigned in the zoomed plot ranged between δ170 to 173ppm for the two generations of sulfur-rich HBPs, SA-G-1-polyol and SA-G-2-polyol. Relative integration of the ester carbonyl carbon signals of S-core monomer for linear (L), dendritic (D) and terminal (T) units were carefully performed as depicted in **Figure SI-7**. In case of SA-G-1-polyol, the NMR signals at δ = 172.54 (D), 172.34 (L), 172.14(T), yielded relative intensities of 0.3, 0.2, and 1.0 respectively. Substituting the contributions in equation (1) as D = 0.3, L = 0.2 and T = 1.0, the estimated degree of branching for SA-G-1-polyol was obtained to be 86.6 %. Similarly, the D, L, and T units of SA-G-2-polyol are observed at δ = 172, 170.5 and 170.12 with relative intensities of 0.1, 0.2, and 1.0, respectively. Thus, with an input of these values in equation (1), the DB of second generation SA-G-2-polyol was assessed to be 84.6%. Interestingly, the findings indicate that with increase in generation, access to the reactive functional groups become progressively difficult leading to an increase in the presence of linear unreacted components within the HBPs.

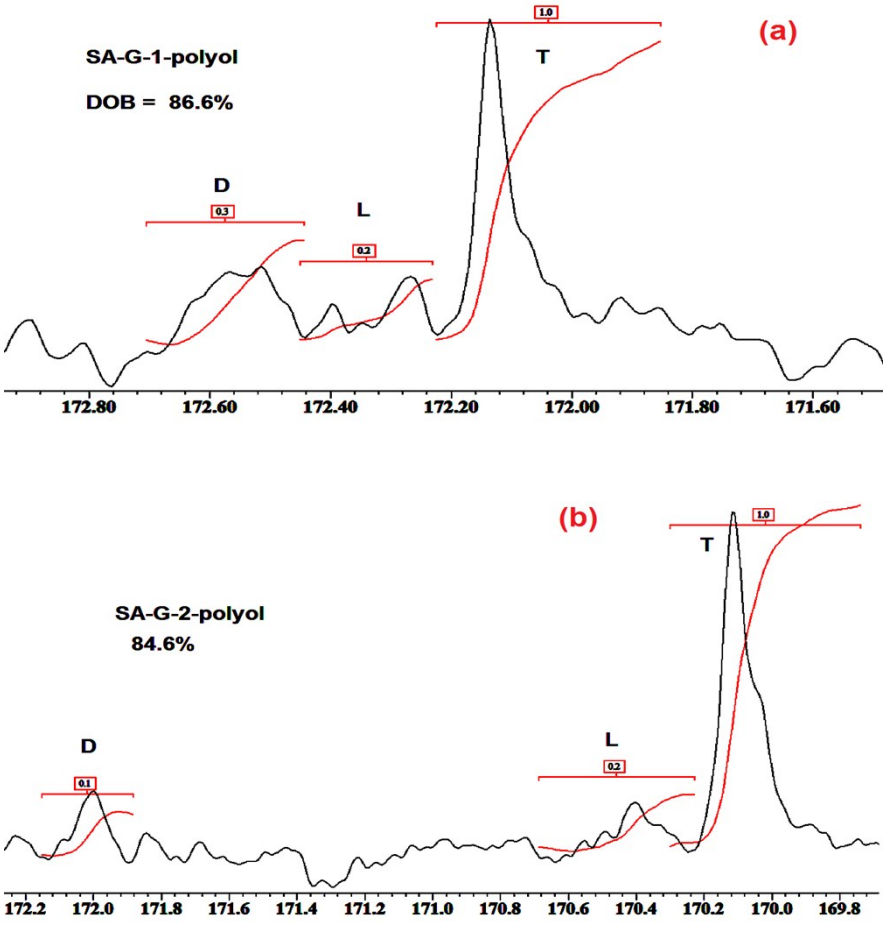

Figure SI-7. Zoomed in ^{13}C-NMR spectra with appropriately assigned D, L and T units for the sulfur-rich HBPs. The relative peak intensities of ester carbonyl carbon present in **(a)** SA-G-1-polyol and **(b)** SA-G-2-polyol were considered for estimating the degree of branching (DOB).

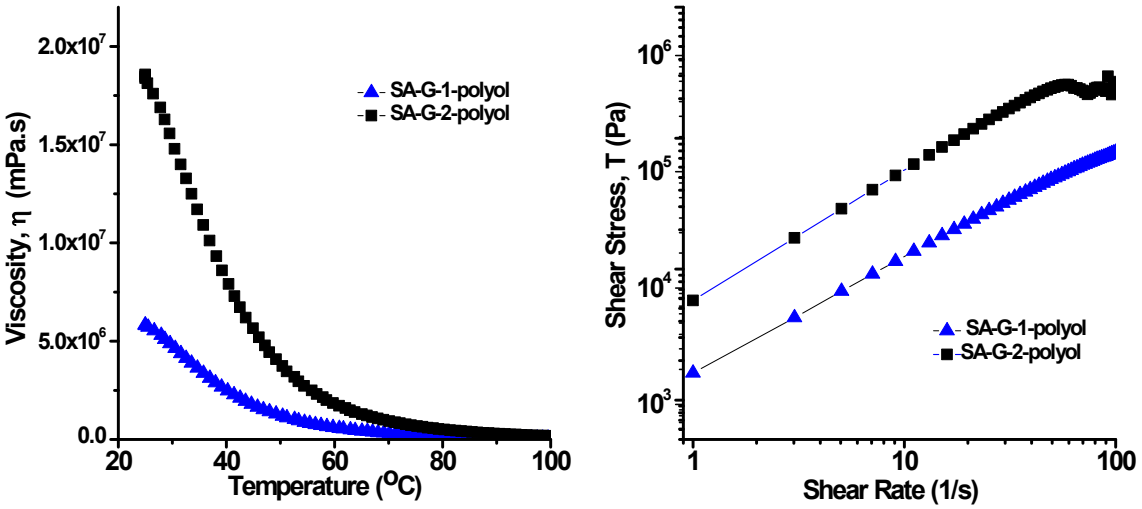

Figure SI-8. (a) Viscosity as a function of temperature for SHBPS. **(b)** flow curves of SHBPs as shear rate vs shear stress.

Table SI-1 Rheological properties of SHBPs (SA-G-1-polyol and SA-G-2-polyol).

Sample	Viscosity (MPa) at			Activation Energy
	30 °C	50 °C	70 °C	kJ/mol
SA-G-1-polyol	4.88	1.19	0.31	57.7
SA-G-2-polyol	17.7	4.25	1.06	59.4

Thermal stability of SHBPs

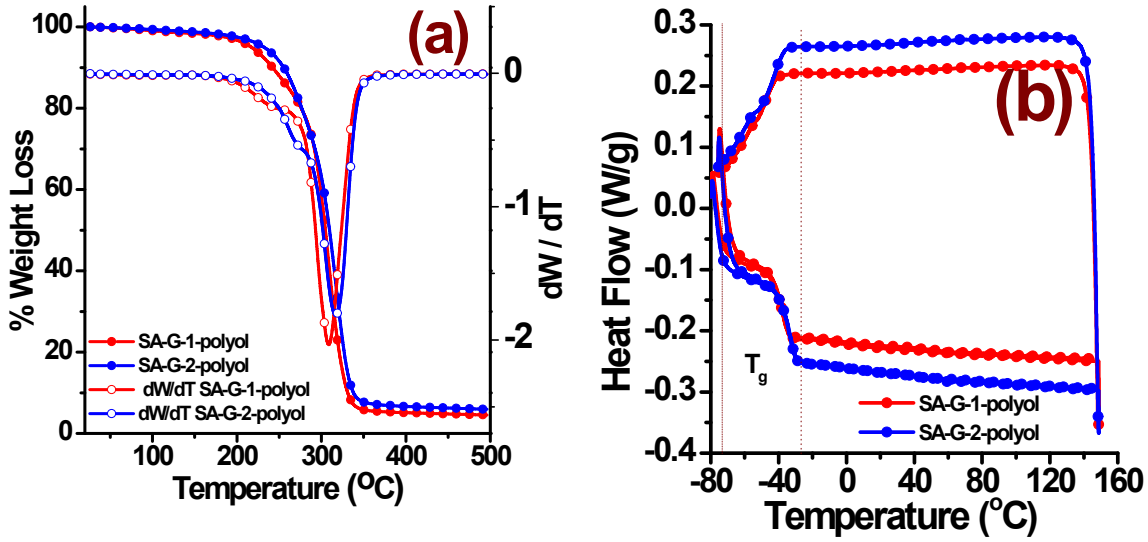

Figure SI-9. Thermal properties of the sulfur-rich HBPs assessed using thermogravimetry (TG) and differential scanning calorimetry (DSC): **(a)** Thermogravimetric profiles along with their corresponding differential plots show primarily single step degradation with a onset temperature of ~ 210 °C indicating high thermal stability; **(b)** DSC thermograms of both the HBPs(SA-G-1-Polyol and SA-G-2-Polyol) revealed low glass transition zones imparting processabilty of polymers at room temperature.

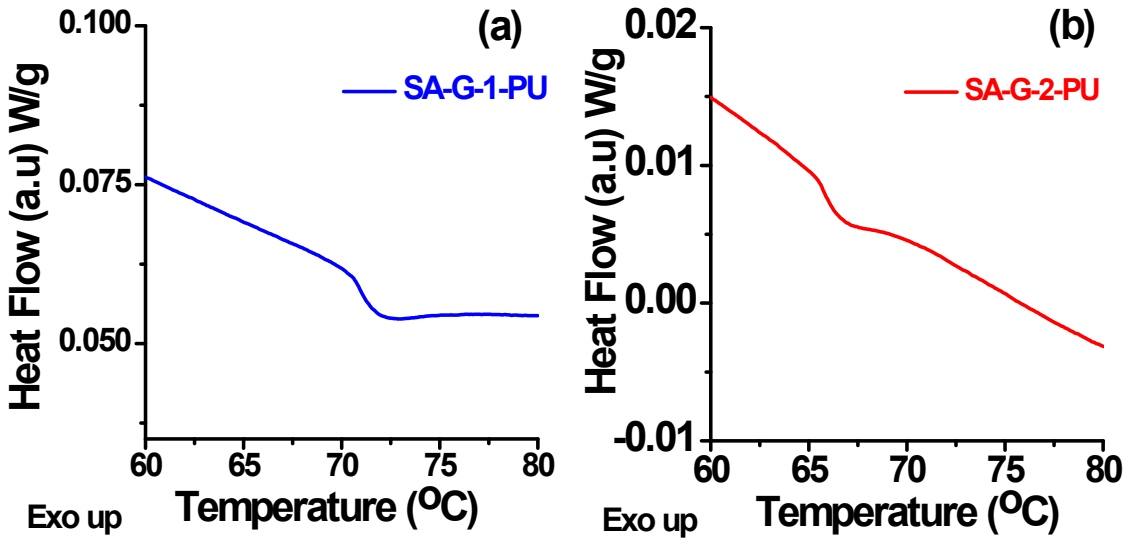

Figure SI-10. Zoomed DSC thermograms of both the PU-urea coatings **(a)** SA-G-1-PU and (**b)** SA-G-2-PU clearly depicting the second glass transition temperatures of the coatings.

Assessing the Antimicrobial Properties of Sulfur-rich PU-Urea Films

The developed sulfur-rich PU-Urea films were undergone to test antimicrobial activity for their feasibility as antimicrobial and antifouling coating applications. Following the standard disk diffusion assay according to the protocol of Conner *et al.*, [7] and Elgayyar *et al.*,[8] in Luria Bertani (LB) agar medium with model strains, tests were carried out on the films. The antibacterial activity was assessed using both gram positive and gram negative bacterial strains. In these tests, *Staphylococcus aureus*, *Bacillus subtilis* were used as gram positive bacterial strain while *Escherichia coli* and *Pseudomonas aeruginosa* as the gram negative. Tests were also performed using two typical fungus: *Aspergillus flavus* and *Saccharomyces cerevisiae*.

The antimicrobial performance of the films was assessed typically in embedded culture. About 5 mL of LB media broth were taken and incubated with the respective strains of bacteria or fungi along with the films. After 48 hours post-incubation, the optical density of the samples was measured to assess the growth of bacteria/fungi. **Figure SI-10** displays that the coatings did not show high zone of inhibition but interestingly they showed good stability in the bacterial/fungi growth with very little zone of inhibition. The second generation coating SA-G-2-PU, in particular, showed relatively better result (slight inhibition zone) against antimicrobial attacks compared to that of first generation SA-G-1-PU coatings.

A plausible reason for the stability/activity exhibited by these PU-Urea films could be rationalized in the following lines. An *in-situ* formation of quaternary ammonium cations (QAC) within the PU-matrix is a strong possibility owing to intermolecular H-bonding mediated by the N-atom in urethane-urea moiety. The charged cationic-site is known to act as an active biocide.[9] Additionally, the activity is also enhanced further by the numerous sulfur atoms present in the polymer backbone and exposed on the surface of the films. SA-G-2-polyol is comparatively less branched than SA-G-1-polyol, thus resulting in SA-G-2-PU with more linear chains present. Generally, antimicrobial activity is also dependent on the number of linear chains and the chain length of HBP arm.[10] Thus, the second generation PU-coatings, SA-G-2-PU not only contains more QACs and sulfur atoms in the matrix but also possess a more open structure that allows more interaction with the broth. Hence, as the generation number of the HBPs is increased its antimicrobial activity is expected to increase. Overall, the findings suggest

that by altering the periphery of the HBPs we can tailor the matrices to optimize the antimicrobial properties and generate antifouling coatings for niche applications.

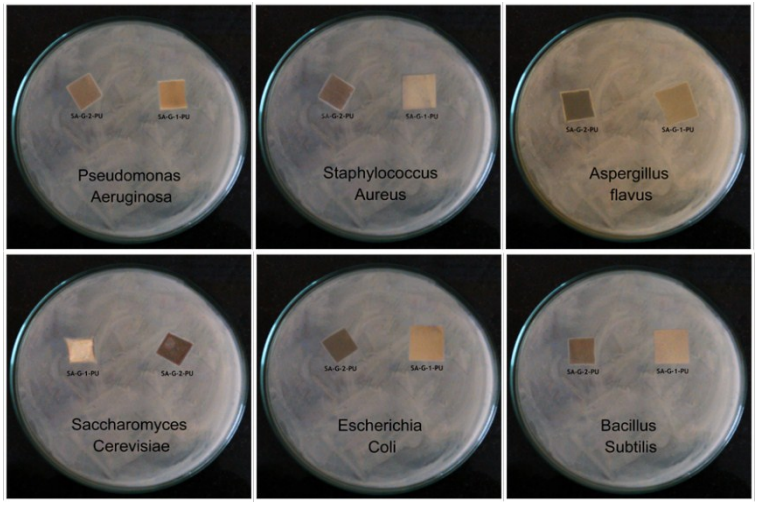

Figure SI-11. Images depicting the stability of SA-G-1-PU and SA-G-2-PU against gram-positive, gram-negative bacteria as well as fungal strains. The antimicrobial activity of SA-G-2-PU is observed to be relatively higher possibly owing to its open architecture and active sites.

References

1. J. F. Stumbé and B. Bruchmann, *Macromol. Rapid Commun.*, 2004, **25**, 921.

2. D. M. Dhevi, A. A. Prabu, H. Kim and M. Pathak, *J. Polym. Res.*, 2014, **21**, 1.

3. G. Bierwagen, D. Tallman, J. Li, L. He and C. Jeffcoate, *Prog. Org. Coat.*, 2003, **46**, 149.

4. M. Stern and A. L. Geary, *J. Electrochem. Soc.*, 1957, **104**, 56.

5. Ch. J. Weng, H. Jane-Yu, H. Kuan-Yeh, J. Yu-Sian, T. Mei-Hui and Y. Jui-Ming, *Electrochim. Acta*, 2010, **55**, 8430.

6. C. E. Hoyle, T. Y. Lee and T. Roper, *J. Polym. Sci., Part A: Polym. Chem.*, 2004, **42**, 5301.

7. D. E. Conner and L. R. Beuchat, *J. Food Sci.*, 1984, **49**, 429.

8. M. Elgayyar, F. A. Draughon, D. A. Golden and J. R. Mount, *J. Food Prot.*, 2001, **64**, 1019.

9. R. Kumar, R. Narayan, T. M. Aminabhavi and K. V. S. N. Raju, *J. Polym. Res.*, 2014, **21**(547), 1–16.

10. T. Ikeda, S. Tazuke and Y. Suzuki, *Makromol. Chem.*, 1984, **185**, 869.